32ND INTERNATIONAL COSMIC RAY CONFERENCE, BEIJING 2011

Observation of the gamma ray source MGRO J1908+06 with ARGO-YBJ

S.VERNETTO[1] AND T.DI GIROLAMO[2] ON BEHALF OF THE ARGO-YBJ COLLABORATION
[1]*INAF-IFSI Torino, and INFN Sezione di Torino, Italy*
[2]*Dipartimento di Fisica dell'Università di Napoli, and INFN Sezione di Napoli, Italy*
vernetto@to.infn.it

Abstract: The gamma ray source MGRO J1908+06 has been observed for 3 years by the ARGO-YBJ experiment at energies above $\sim$1 TeV. According to our data the source is extended, and parametrizing the shape with a two–dimensional Gaussian we estimate an extension σ_{ext} = 0.50° $\pm$ 0.35°. The large size of the emitting region supports the identification of the source as the Wind Nebula associated with the Fermi pulsar PSR J1907+0602. The energy spectrum obtained is dN/dE = 2.2$\pm$0.4 $\times$ 10^{-13} (E/7 TeV)$^{-2.3\pm0.3}$ photons cm^{-2} s^{-1} TeV^{-1}, in the range $\sim$2-30 TeV. The flux is in good agreement with the results of the Milagro detector, but is $\sim$3 times larger than what has been obtained by the Cherenkov Array H.E.S.S.. The origin of these disagreements remains unclear, but it could be due to a complex morphology of the source and/or to the contribution of the diffuse gamma ray flux from the Galactic plane.

Keywords: MGRO J1908+06, Pulsar Wind Nebula, Supernova Remnant

1 Introduction

The extended gamma ray source MGRO J1908+06 has been discovered in 2007 by the Milagro air shower detector in a survey of the Galactic plane at a median energy of $\sim$ 20 TeV [1]. The source was later observed by H.E.S.S. [2] and VERITAS [3]. In particular, H.E.S.S. measured a power law energy spectrum with a photon index of 2.10 $\pm$ 0.07$_{stat}$ $\pm$ 0.2$_{sys}$ in the energy range 0.3-20 TeV, corresponding to an integral flux of 0.17 Crab units above 1 TeV. Assuming a Gaussian shape for the source, H.E.S.S. evaluated an extension of σ_{ext} = $0.34^{\circ}{}^{+0.04}_{-0.03}$.

The proximity of MGRO J1908+06 to the Fermi LAT pulsar PSR J1907+0602, lying at a distance $\sim$14' from the centroid of the H.E.S.S. source, suggested to identify it with the Wind Nebula of the pulsar [4, 5]. Performing an off-pulse measurement, Fermi set an upper limit to the nebula flux in the energy region 0.1-25 GeV, showing that the spectrum has a low-energy turnover between 20 GeV and 300 GeV. With radio and X-ray data, a lower limit to the pulsar distance was set to $\sim$3.2 kpc, deriving for the nebula a physical size $\geq$40 pc.

Finally Milagro evaluated the energy spectrum in the 2-100 TeV energy region, reporting a very hard power law spectrum with an exponential cutoff [6]. The best fit obtained is dN/dE = 0.62 $\times$ 10^{-11} E$^{-1.50}$ exp(-E/14.1) photons TeV^{-1}cm^{-2}s^{-1}, with E in TeV. This flux is in disagreement with that given by H.E.S.S. by $\sim$2-3 standard deviations, being about a factor 3 higher at 10 TeV. The authors suggest that the discrepancy can be simply due to a statistical fluctuation, or to the fact that Milagro, given its relatively poor angular resolution, integrates the signal over a larger solid angle compared to H.E.S.S., and likely detects more of the diffuse lateral tails of the extended source.

In this work we report on the observation of MGRO J1908+06 with the ARGO-YBJ detector performed during $\sim$3 years, with our evaluation of the extension and the energy spectrum.

2 The ARGO-YBJ experiment

The ARGO-YBJ detector consists of a $\sim$74$\times$ 78 m^2 carpet made of a single layer of Resistive Plate Chambers (RPCs) with $\sim$93% of active area, sorrounded by a partially instrumented ($\sim$20%) area up to $\sim$100$\times$110 m^2. The apparatus has a modular structure, the basic data acquisition element being a cluster (5.7$\times$7.6 m^2), made of 12 RPCs (2.8$\times$1.25 m^2). The RPCs are operated in streamer mode by using a gas mixture (Ar 15%, Isobutane 10%, TetraFluoroEthane 75%) suitable for high altitude operation. Each RPC is read by 80 strips of 6.75$\times$61.8 cm^2 (the spatial pixels), logically organized in 10 independent pads of 55.6$\times$61.8 cm^2 which are individually acquired and represent the time pixels of the detector [7]. In addition, in order to extend the dynamical range up to PeV energies, each RPC is equipped with two large size pads (139 $\times$ 123 cm^2) to collect the total charge developed by the particle hitting the detector [8]. The full experiment is made of 153 clusters for a total active surface of $\sim$6600m^2.

ARGO-YBJ operates in two independent acquisition modes: the *shower mode* and the *scaler mode* [9]. In this analysis we refer to the data recorded in shower mode. In this mode, an electronic logic has been implemented to build an inclusive trigger, based on a time correlation between the pad signals, depending on their relative distance. In this way, all the shower events giving a number of fired pads $N_{pad} \geq N_{trig}$ in the central carpet in a time window of 420 ns generate the trigger. The current trigger condition is N_{trig}=20, corresponding to a rate of 3.5 kHz and a dead time of 4%.

The time and the location of each fired pad are recorded and used to reconstruct the position of the shower core and the arrival direction of the primary particle [10]. In order to perform the time calibration of the 18360 pads, a software method has been developed [11].

The angular resolution and the pointing accuracy of the detector have been evaluated by using the Moon shadow, i.e. the deficit of cosmic rays in the Moon direction[12]. The shape of the shadow provides a measurement of the detector Point Spread Function (PSF), and its position allows the individuation of possible pointing biases. The data have been compared to the results of a Monte Carlo simulation of the propagation of cosmic ray in the Earth magnetic fields, the shower development in the atmosphere by using the CORSIKA code [13], and the detector response with a code based on the GEANT package [14]. The PSF measured with cosmic rays has been found in excellent agreement with the Monte Carlo evaluation, confirming the reliability of the simulation procedure.

The Moon shadow has been also used to check the absolute energy calibration of the detector, by studying the westward shift of the shadow due to the geomagnetic field. The observed displacement as a funcion of the event multiplicity N_{pad} is as well in agreement with the simulation. From this analysis the total absolute energy scale error, including systematics effects, is estimated to be less than 13%

With the same simulation codes we evaluated the angular resolution for gamma rays, that results smaller with respect to protons by ∼30-40% depending on N_{pad}, due to the better defined time profile of the showers. For events with $N_{pad} \geq 40$ the PSF can be described by the sum of two Gaussian distributions, the radius of the opening angle that maximizes the signal to background ratio is 1.1° and contains 55% of the signal.

3 Data analysis

The dataset used in this analysis contains all the showers with zenith angle less than 45° and $N_{pad} \geq 40$, where N_{pad} is the number of hit pads on the central carpet.

To study the gamma ray emission from a source, a 8°×8° sky map in celestial coordinates (right ascension and declination) with 0.1°×0.1° bin size, centered on the source position, is filled with the detected events. In order to extract the excess of gamma rays, the cosmic ray background is estimated using the *time swapping* method [15] and it is used to build a "background map".

The maps are then "integrated" over a circular area of radius ψ_{max}, i.e. every bin is filled with the content of all bins whose center has an angular distance less than ψ_{max}, where the ψ_{max} values are chosen according to simulations in order to maximize the signal to noise ratio, and will be discussed later. Finally, the integrated background map is subtracted to the integrated event map, obtaining the "excess map", where for every bin the statistical significance of the excess is calculated.

In case of a positive detection (i.e. a statistically significant excess in the central bin), to study the energy dependence of the signal the events are divided in different subsets according to the number of hit pads, and the above procedure is carried out for each N_{pad} interval. The source spectrum is then evaluated by means of a simulation, by comparing the number of excess events detected in the central bin of the map for each N_{pad} interval, with the corresponding values expected assuming a set of test spectra. The expected rates are obtained by a Monte Carlo procedure that simulates the events from a gamma ray source with a given spectrum and following a given daily path in the sky. The reliability of this procedure has been tested studying the Moon shadow deficit [12], the Crab Nebula [16] and Mrk421 signals [17].

Given an input spectrum, the simulation output also provides for each N_{pad} interval the values of the angular window radius ψ_{max} that maximize the signal to noise ratios, and the corresponding "efficiency" ϵ, i.e. the fraction of source events contained in this window.

For a point source, given a N_{pad} interval, the value of ψ_{max} is related to the PSF, that depends both on the detector characteristics and on the source spectrum. The spectral shape determines the distribution of both N_{pad} and the shower core position, crucial parameters in the reconstruction of the arrival directions. In case of an extended source the value of ψ_{max} also depends on the intrinsic angular extension and on the shape of the source. The Monte Carlo simulation also provides the values of ψ_{max} for a source with a given extension and shape.

From the experimental point of view, if the extension is unknown, one should first determine it in order to evaluate the correct windows to extract the signal for the spectrum. On the other hand, to evaluate the extension one has to study the angular distribution of the events around the source, that also depends on the PSF, that in turn depends on the spectrum. In conclusion, the spectrum and the extension cannot be independently determined. To solve this "circular" problem an iterative procedure is necessary,

For simplicity we assume a source with a shape described by a symmetrical bidimensional Gauss function with r.m.s. = σ_{ext}, independent of the gamma ray energy. For the spectrum we assume a power law dependence: $dN/dE = K\, E^{-\gamma}$.

The iterative procedure to determine the spectral parameters K and γ and the extension σ_{ext} is based on two steps.

In the first step, assuming a spectrum slope (γ= 2.5 in the first iteration), the angular spread of the events around the source position is studied to evaluate the extension σ_{ext}. The number of detected events as a function of the angular distance from the source (in bins of Δr=0.5°, from 0° to 3°) is compared with a set of simulated distributions, obtained varying the value of σ_{ext} (from 0° to 2°, in steps of 0.01°) and the value of a normalization parameter N in a convenient range. For each tested distribution, the χ^2 is calculated to find the values of σ_{ext} and N that best fit the data.

In the second step, the event rates observed in different N_{pad} intervals are studied to determine the spectrum. We define 4 N_{pad} intervals: 40-99, 100-299, 300-999 and $\geq$1000, and for each of them we evaluate the number of events in the observational window. The radii of the windows ψ_{max} are given by the simulation assuming the source extension and the spectral slope of the previous step. The observed event rates are corrected for the corresponding efficiencies ϵ of the windows. A further correction of the order of a few per cent is made to take into account the small overestimation of the background due to the time swapping method.

The observed rates are finally compared with those expected by a set of simulated test spectra, varying the spectral index γ and the normalization parameter K. The best parameters are found by minimizing the χ^2.

The obtained spectral slope γ is returned to the first step, to recalculate a new extension and successively a new spectrum, and so on, until the convergence of the parameters is reached.

Given the relatively weak dependence of the PSF on the spectrum slope, a small number of iterations is sufficient to terminate the process successfully.

4 Results and discussion

At the ARGO-YBJ site, MGRO J1908+06 culminates at the zenith angle of 24° and is visible for 5.4 hours per day with a zenith angle less than 45°. The dataset used in this analysis refers to the period from November 2007 to February 2011. The total on-source time is 5358 hours.

Fig.1 shows the ARGO-YBJ sky map for events with N_{pad} >40. An area of excesses with statistical significance larger than 4-5 s.d. is evident around the location of the H.E.S.S. source.

Centering on the H.E.S.S. source, the iterative procedure described in the previous section gives for the extension the value σ_{ext}=0.50°$\pm$0.35, consistent with the H.E.S.S. measurement, while the obtained energy spectrum is:

dN/dE = 2.2$\pm$0.4 $\times$ 10^{-13} (E/7 TeV)$^{-2.3\pm0.3}$ photons cm^{-2} s^{-1} TeV^{-1}, with a χ^2 value of 0.17 for 2 degrees of freedom (the errors on the fit parameters are statistical).

Beside the statistical errors, this measurement could be affected by a systematic uncertainty of $\leq 30\%$ mainly due to the background evaluation and to the determination of the absolute energy scale.

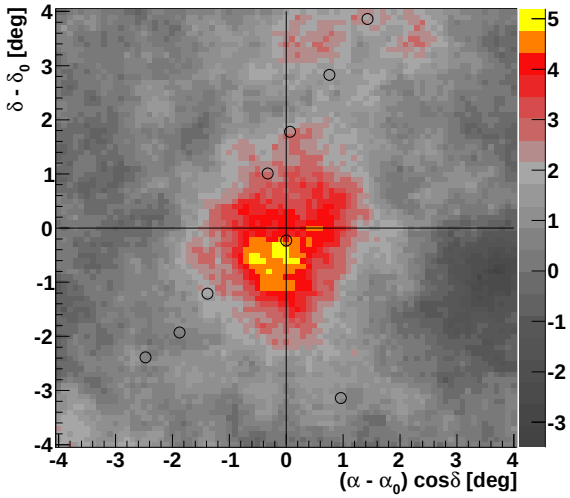

Figure 1: Significance map of the MGROJ1908+06 region obtained by ARGO-YBJ, for events with N_{pad} >40. The events of the map have been smoothed with a window radius ψ_{max}=1.5°, to optimize the signal to noise ratio for this extended source. The map is centered on the position of H.E.S.S. source centroid (α=286.98°, δ=6.27°). The open circles show the positions of the gamma ray sources observed by Fermi in the same region [18].

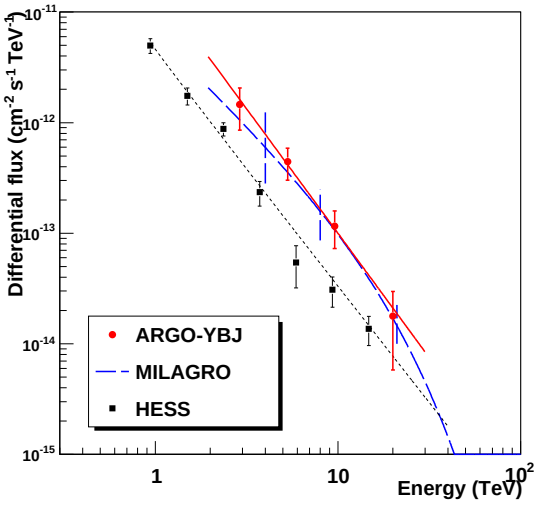

Figure 2: Gamma ray flux from MGRO J1908+06 measured by different detectors: 1) ARGO-YBJ: filled circles. The continuous line is the best fit to data. 2) Milagro: the dashed line is the spectrum fit and the superimposed vertical lines are the errors (at 1 s.d.) for some values of the energy. 3) H.E.S.S.: squares. The dotted line is the best fit. The plotted errors are purely statistical for all the detectors.

The spectrum (Fig.2) is in agreement with Milagro, but only marginally consistent with H.E.S.S., being the ARGO-YBJ flux a factor $\sim$3 larger. The origin of such a disagreement could be a statistical fluctuation and/or the effect of systematic uncertainties (H.E.S.S. reports a systematic error of $\sim$20% on the flux). However, since a higher flux has been observed also by Milagro, it is worthwhile to suggest different possibilities.

A possibility is that the larger flux measured by the ARGO and Milagro detectors is the consequence of the contamination of other extended sources lying near the object observed by H.E.S.S., since the former detectors have a worse angular resolution and integrate the signal over a larger area. Fig.1 shows the positions of all the gamma ray sources detected by Fermi in the same region (all of them unidentified except PSR J1907+0602), according to the Fermi First Catalogue [18]. A few of them, if associated with extended TeV nebulae, could in principle contribute to the observed signal, lying at a distance less than $\sim 2^\circ$-3° from MGRO J1908+06. Their contribution however should be small, since the ARGO-YBJ excess is consistent with the position of PSR J1907+0602.

A larger contribution is expected from the diffuse gamma ray flux produced by cosmic rays interacting with matter and radiation in the Galaxy. According to the prediction of the "optimized" GALPROP model [19, 20], confirmed by a MILAGRO measurement at 15 TeV [21], the amount of this contribution to the measured flux from MGRO J1908+06 at a few TeV can be of the order of 15-20%, and cannot account for the entire observed disagreement.

A complex morphology of the source could also affect the flux measurement. Both ARGO-YBJ and H.E.S.S. use a one-parameter Gaussian to model the shape of the emission region, that could be insufficient for a description of the source, producing some biases.

Finally, one cannot exclude the possibility of a flux variation as the origin of the observed disagreement among the detectors. In fact Milagro, H.E.S.S. and ARGO-YBJ data have been recorded in different periods. Milagro integrates over seven years (July 2000 - November 2007) while the total H.E.S.S. data set only amounts to 27 hours of observation during 2005-2007, before the ARGO-YBJ data. However, a temporal analysis of the ARGO-YBJ data has shown that the signal, in the limit of the detector sensitivity, is consistent with a stable flux, on time scales ranging from a few days to months. Morevover, it should be noted that the MGRO J1908+06 emission, differently from that of the Crab Nebula, originates from a region large $\geq$40 pc, implying that the variation time scale cannot be less than $\sim$130 years, unless relativistic beaming effects are present.

So far, the problem remains open. The collection of higher statistics by continuously monitoring MGRO J1908+06, should lead to the solution of this question.

References

[1] Abdo, A.A. et al. 2007, ApJL 664, L91
[2] Aharonian F. et al. 2009, A&A, 499, 723
[3] Ward, J.E. et al. 2008, in AIP Conf. Proc. 1085, High energy Gamma-Ray Astronomy, ed. F.A. Aharonian, W. Hofmann, & F.Rieger (Melville. NY:AIP), 301
[4] Abdo, A.A. et al. 2009, ApJL 700, L27
[5] Abdo, A.A. et al. 2010, ApJ 711, 64
[6] Smith, A.J., et al. 2010, Proc. Fermi Symposium, Washington, D.C, 2009 Nov. 2-5 (arXiv:1001.3695)
[7] Aielli, G. et al. 2006, NIM A, 562, 92
[8] Iacovacci, M., et al. 2009, Proc. 31st ICRC, Lodz, Poland
[9] Aielli, G., et al. 2008, Astrop. Phys., 30, 85
[10] Di Sciascio, G., et al. 2007, Proc. 30th ICRC, Merida, Mexico (arXiv:0710.1945)
[11] Aielli, G., et al. 2009, Astrop. Phys., 30, 287
[12] Di Sciascio, G., et al. 2010, Proc. 8th Workshop on Science with the new generation of high energy gamma-ray experiments, Trieste, Italy (arXiv:1012.4400)
[13] Heck, D., Knapp, J., Capdevielle, J.N., Shatz, G., & Thouw, T. 1998, Forschungszentrum Karlsruhe Report No. FZKA 6019
[14] GEANT - Detector Description and Simulation Tool 1993, CERN Program Library, W5013
[15] Alexandreas, D.E., et al. 1993, NIM A, 328, 570
[16] Vernetto, S., et al. 2011, these proceedings
[17] Aielli, G., et al., 2010, ApJL 714, L208
[18] Abdo, A.A. et al. 2010, ApJS 188, 405
[19] Strong, A.W., Moskalenko, I.V., Reimer, O. 2000, ApJ, 537, 763
[20] Porter, T.A., Moskalenko, I.V., Strong, A.W., Orlando, E., & Bouchet, L. 2008, ApJ 682, 400
[21] Abdo, A.A. et al. 2008, ApJL 688, 1078